JOURNAL OF OPTOELECTRONICS AND ADVANCED MATERIALS, Vol. 12, No. 7, July 2010, 1590 - 1596

Corrosion behaviour of some titanium dental alloys synthesized by cold crucible levitation melting

D. MARECI, R. CHELARIU[a], G. CIURESCU, D. SUTIMAN[*], D. M. GORDIN[b], T. GLORIANT[b]
"Gh. Asachi" Technical University of Iasi, Faculty of Chemical Engineering and Environmental Protection, 71 Mangeron Blvd., 700050, Iasi, Romania,
[a]*"Gh. Asachi" Technical University of Iasi, Faculty of Materials Science and Engineering, 59 Mangeron Blvd., 700050, Iasi, Romania*
[b]*INSA Rennes, UMR CNRS 6226 Sciences Chimiques de Rennes/ Chimie-Metallurgie 20 avenue des buttes de Coesmes, F-35043, Rennes cedex, France*

Corrosion behaviour of the studied Ti12Mo and Ti12Mo5Ta alloys together with the currently used metallic biomaterials commercial pure titanium (cp-Ti) were investigated for dental applications. All the samples were examined using electrochemical techniques: open circuit potential, potentiodynamic polarization curves and electrochemical impedance spectroscopy (EIS) in artificial saliva at 25 ^{o}C. The electrochemical corrosion properties of all the titanium samples in artificial saliva were measured in terms of zero current potential (ZCP) and corrosion current density (i_{corr}). The EIS technique was applied to study the nature of the passive film formed on all the samples at various impressed potentials: 0 V (SCE), 0.5 V (SCE) and 1 V (SCE). Equivalent circuits (EC) were used to modeling EIS data, in order to characterize samples surface and better understanding the effect of Mo and Ta addition on the cp-Ti.

(Received May 15, 2010; accepted July 14, 2010)

Keywords: Titanium samples, Potentiodynamic polarization, SEM, EIS, passive films

1. Introduction

Titanium and its alloys have become ones of the most attractive biomaterials to make orthopedic implants, dental implants, and other devices for dental applications due to low density, high specific strength, and elastic modulus closer from the one of the bone tissue, and superior corrosion resistance in body fluids [1-9]. On the surface of the titanium and its alloys a stable, adherent, compact and passive layer, consisting principally of TiO_2 oxide, is naturally formed. This titanium oxide being an n-type semiconductor has only ionic conductivity, and it is responsible for the high corrosion resistance of titanium and its alloys in various electrochemical media [10, 11]. Also, oxide layer has an important role in point of the biocompatibility of titanium-based biomaterials [12].

Ti6Al4V alloy (ASTM F-1472, ASTM F-136, ISO 5832-3) and V free α+β type alloys such as Ti6Al7Nb (ASTM F-1295, ISO 5832-11) and Ti5Al2.5Fe (ISO 5832-10) have been used in dentistry [13, 14]. Further studies have indicated that V, used to stabilize the β-phase, produces harmful oxides for the human body [15-17]. According to Piazza et al. [18], Al is poorly absorbed within the gastrointestinal tract, very little gets into the blood stream, but has been concerned, not yet confirmed, about the association between Al and Alzheimer disease [19, 20]. For this reason, novel titanium alloys with greater biocompatibility and lower elastic modulus are desirable. More recently metallic biomaterials research has focused on the β type titanium alloys with excellent biocompatibility and biomechanical properties (low elastic modulus) [21, 22]. The β-stabilizing elements, such as Ta, Zr, Mo and Sn are selected as safe alloying elements to titanium, which are judged to be non-toxic and non-allergic [23].

Molybdenum is used as alloying element for titanium because has a good thermodynamic stability [24, 25]. Mo is considered to be instrumental in regulating the pH balance in the body and act as a cofactor for a limited number of enzymes in humans [26, 27]. Ti15Mo (%wt.) alloy is actually standardized (ASTM F 2066) [28], in recent years Ti10Mo (%wt.) [29], Ti(4÷20)Mo (%wt.) [30, 31] were also investigated in view of biomedical and dental applications. Tantalum is considered as one of the best biocompatible in human body [32] but have a relatively high cost. Recently the Ti-Ta alloys were developed [9, 22, 33-35], and they are expected to become promising candidates for biomedical applications.

The stability of the β-phase in the case of titanium alloys is expressed as the sum of the weighted averages of the alloying elements in wt.% known as the Mo equivalent [36-38]. If this parameter has a value less than 8 wt.%, the alloy usually exhibits a martensitic transformation when quenched from temperatures above the β transus. A value of Mo equivalent being approximately in the range 8–24 wt% indicates β-metastable titanium alloys because the β-stabilizers content is high enough to prevent any martensitic transformation in the β phase upon quenching to room temperature [36, 37, 39].

Electrochemical reactions are one of the most important interactions between dental alloys and oral fluids. The modifications of the dental alloys properties could be determined using rapid electrochemical tests to estimate the corrosion resistance [40, 41].

The aim of the present study was to investigate the effect of Mo and Ta addition on the electrochemical corrosion behaviour of the commercial pure titanium (cp-Ti) in artificial saliva.

2. Materials and methods

2.1. Materials

The origin and nominal chemical compositions of the titanium samples studied are shown in Table 1.

Table 1. Origin and chemical composition of investigated titanium samples.

Samples	Nominal Chemical Composition (wt %)	Supplier
cp-Ti	Ti: 99.9	IMNR, Romania*
Ti12Mo	Ti: 88, Mo: 12	INSA Rennes, France**
Ti12Mo5Ta	Ti: 83, Mo: 12, Ta: 5	INSA Rennes, France

*National Institute of Research & Development for Non-ferrous and Rare Metals, Bucharest, Romania; ** INSA Rennes, France.

Both Ti12Mo and Ti12Mo5Ta alloys were synthesized using the procedure described elsewhere [42, 43]. Using the equation of Mo equivalent indicated in literature [36, 38, 44], the Mo equivalent values of the investigated alloys are 12 for Ti12Mo, and 13.1 for Ti12Mo5Ta. This indicates that both titanium alloys are β-metastable with similar structural characteristics.

The cp-Ti samples were obtained from a bar stock in annealed state. The structural characterization of the cp-Ti was detailed elsewhere [45].

The samples were cut into 0.19 cm^2 sizes and brass nut was attached to sample using conductive paint to ensure electrical conductivity. The assembly was then embedded into an epoxy resin disk. Then the samples were ground with SiC abrasive paper up to 2000 grit, final polishing was done with 1 μm alumina suspension. The samples were degreased with ethyl alcohol followed by ultrasonic cleaning with deionised water and dried under a hot air stream.

2.2. The corrosion media

Fusayama artificial saliva was selected as it has been shown to produce results that were consistent with the clinical experience of dental alloys [46]. Fusayama artificial saliva [47] was prepared immediately before being used and consisted of: 0.400 g NaCl; 0.400 g KCl; 0.795 g $CaCl_2 \cdot 2H_2O$; 0.780 g $NaH_2PO_4 \cdot 2H_2O$; 0.005 g $Na_2S \cdot 9H_2O$; 1.000g NH_2CONH_2 and distilled water up to 1000 mL. The pH was measured with a multiparameter analyzer CONSORT 831C. The pH of this saliva was 5.6.

2.3. Electrochemical tests

Electrochemical measurements were carried out in aerated solution at 25 ^oC using a Princeton Applied Research potentiostate (Model 263 A) connected with a Princeton Applied Research 5210 lock-in amplifier controlled by a personal computer and a specific software package called Electrochemistry Power Suite (Princeton Applied Research). A glass corrosion cell kit with a platinum counter-electrode and a saturated calomel reference electrode (SCE) were used to perform the electrochemical measurements. All potentials referred to in this article are with respect to SCE.

The cathodic treatment was carried out at –1.5 V for 60 s to remove any oxide films present on the surface of each specimen. After the open-circuit potential (E_{OC}) of each specimen was recorded for one hour, the potentiodynamic polarization curve was performed by stepping the potential using a scanning rate of 10 mV/s [48] from −0.6 V to +1.2 V and reversed in the negative direction to +0.6 V. PowerCorr software (PAR, USA) directly supplies the values of zero current potential (ZCP) and corrosion current densities (i_{corr}). The potentiodynamic test was repeated three times for each specimen.

Electrochemical impedance spectroscopy (EIS) measurements were performed in artificial saliva at different potentials (0 V, 0.5 V and 1 V) at 25 ^oC. EIS results at different potentials were obtained 30 minutes after the overpotential has been applied. The EIS spectra were recorded in the 10^{-2} Hz to 10^5 Hz frequency range. The applied alternating potential signal had amplitude of 10 mV. In order to supply quantitative support for discussions of these experimental EIS results, an appropriate model (ZSimpWin-PAR, USA) for equivalent circuit (EC) quantification has also been used. For titanium oxide films, a distributed relaxation feature was observed [3]. Due to this fact, in this study a constant phase elements (CPE) was used in the fitting procedure to obtain good agreement between the simulated and experimental data instead of an ideal capacitor. The impedance of the CPE is given by [49]:

$$Q = Z_{CPE} = \frac{1}{C(j\omega)^n} \quad (1)$$

where for n = 1, the Q element reduces to a capacitor with a capacitance C and, for n = 0, to a simple resistor. The n is related to a slope of the $Log(Z_{mod})$ vs. Log(Frequency) Bode–plots, ω is the angular frequency and j is imaginary number. The quality of fitting to the EC was judged first by the χ^2 value that was $< 5 \times 10^{-4}$ and second by the error distribution versus frequency comparing experimental with simulated data.

2.4. SEM microscopy of corroded surfaces

In order to observe the occurrence of the surface effects of the corrosion, the some corroded surfaces were

observed by SEM microscopy. To perform this Vega Tescan scanning electron microscope (model VEGA II LMH) having detector (model xflash, Bruker) for EDX analysis, was used.

3. Results and discussion

The intra-orally temperature widely fluctuates because of ingestion of hot or cold food and beverage. Furthermore, different areas of oral cavity exhibited different temperature. Nevertheless, it can be reasonably approximated in experimental settings between 35 ^{o}C and 37 ^{o}C if we considered the environmental temperature as 25 ^{o}C [50].

The open circuit potential is the potential at which the material is in equilibrium with the specific environment. The open circuit potential of a metal varies as function of the time. Figure 1 present the variation of open circuit potential (E_{OC}) for the samples as function of exposure time in artificial saliva. Prior to each measurement, the samples were cathodically polarized at –1.5 V in the working solution for 60 s, in order to remove any spontaneously formed surface film. Open circuit potential variation is similar for all the samples in artificial saliva.

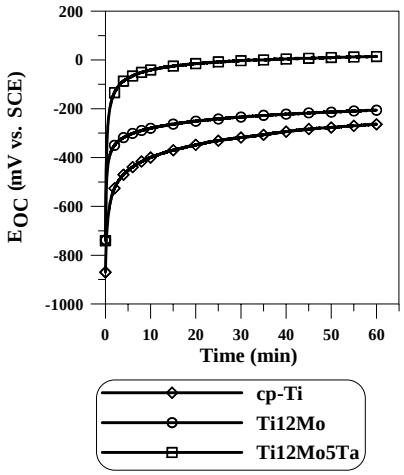

Fig. 1. Variation of open circuit potential (E_{OC}) with time for titanium samples in artificial saliva

From the Fig. 1 all the samples have a tendency to form a passive film by the shift of E_{OC} to more positive (noble) direction with respect to time. An abrupt E_{OC} displacement towards positive potentials was noticed in Figure 1 during a period of 10 minutes. This initial increase seems to be related to the formation and thickening of the oxide film on the metallic surface. Afterwards, the E_{OC} increases slowly suggesting the growth of the oxide film. The protecting of the oxide film increased the corrosion resistance. Stable potentials in open circuit measurements is obtained after one hour exposure in artificial saliva, which means the oxide film become stable. The E_{OC} is determined by both the anodic and cathodic reaction, according to the mixed theory. Decrease of the anodic dissolution current move the E_{OC} in the positive direction. Open circuit potentials for Ti12Mo and Ti12Mo5Ta alloys in artificial saliva are more positive than for cp-Ti, probable due to the positive contribution of the Mo and Ta alloying elements in the formation of oxide film.

3.1 Potentiodynamic polarization

Plots in semi-logarithmic scale of current densities corresponding to all samples after one hour in artificial saliva traced between –0.6 V to +1.2 V and reverse to +0.6 V are displayed in Figures 2. All curves present the same feature. Standard procedures were used to extract "zero current potential" (ZCP) and corrosion current densities (i_{corr}) values from the potentiodynamic polarization plots. The average values of ZCP and i_{corr} determined by the PowerCorr software (PAR, USA) are presented in Table 2. By comparing with data from Table 2, we can notice that in all cases the values determined for the ZCP, are more negative than those corresponding to E_{OC}. The change is probably due to depassivation phenomena on the surface during cathodic scanning.

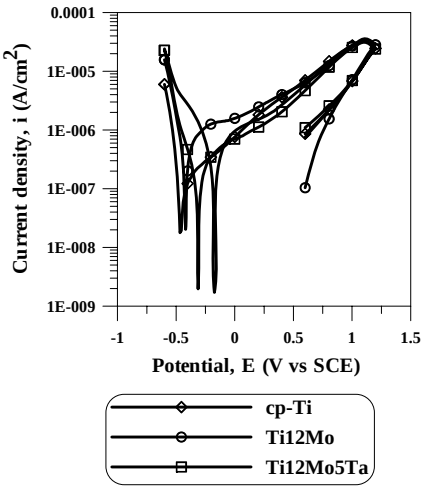

Fig. 2. Potentiodynamic polarisation curves of titanium samples tested after 1 hour maintained in artificial saliva, on semi-logarithmic axes

Table 2. The main parameters of the corrosion process measured for the Ti samples in artificial saliva, at 25 ^{o}C

Samples	ZCP (mV)	i_{corr} ($\mu A/cm^2$)
cp-Ti	-455 ± 19	0.75 ± 0.06
Ti12Mo	-420 ± 16	0.65 ± 0.06
Ti12Mo5Ta	-310 ± 14	0.52 ± 0.05

Very low corrosion current densities (in the order of $10^{-7}A/cm^2$) were obtained from the polarization curves, indicating a high resistance for all the samples in artificial saliva. A comparison of the obtained values with published data is also difficult since the corrosion and

anodic current densities of titanium samples depend on potential scanning rate, surface preparation, heat treatments, and even on exposure time. For all the samples, the potential sweep in positive direction shows an anodic current starting at negative potential that corresponds to the formation of titanium oxides [51-54].

The current exhibited negative hysteresis when the scan was reversed. Figure 3 show, typical SEM images of the resulting surface oxide films after anodic polarization in artificial saliva for Ti12Mo and Ti12Mo5Ta alloys. A homogeneous oxide layer is developed at the surface of the both alloys sample. No pitting or cracks appeared on the alloy surfaces after anodic polarization test.

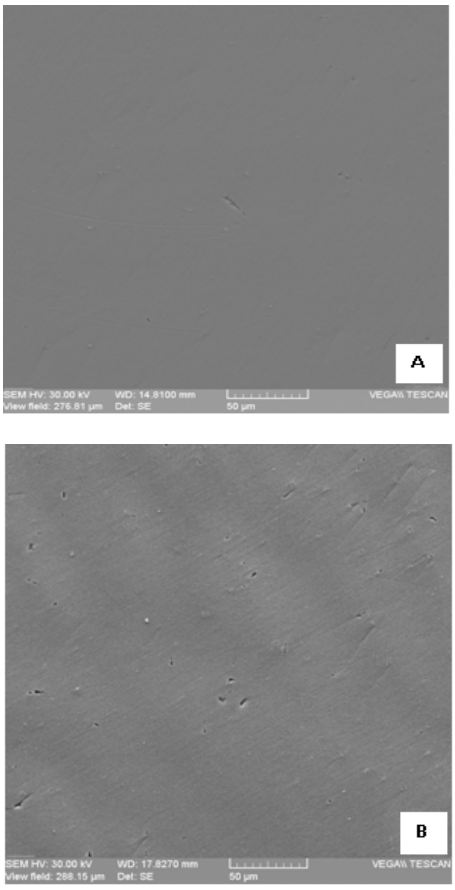

Fig. 3. SEM observations of: (A) Ti12Mo alloy and (B) Ti12Mo5Ta alloy after anodic potentiodynamic polarization tests in artificial saliva

From Table 2 slow differences can be observed for different samples with different alloying element, immersed in artificial saliva. Conventional electrochemical techniques (DC) do not allow distinguishing these influences. To make clear the effect of alloying element, EIS was performed.

From the EIS data we can obtain information about the passive film characteristics. The potentials for investigation of the electrochemical behaviour by EIS measurements for the samples were chosen from above anodic polarisation curve. It was decided to perform these tests at the 0 V, 0.5 V and 1 V.

Impedance spectroscopy results for samples in artificial saliva at selected potential values are presented as Bode plots (Fig. 4(a-c)).

The phase angle maximum observed for all the samples was found to lie in the range of approximately –70^o to –80^o. The values of the phase angle maximum span three frequency decades (0.1 Hz to 100 Hz), gradually decreases with decreasing frequency (below 0.1 Hz). High impedance values (order of 10^6 Ω cm^2) were obtained from medium to low frequencies for these samples suggesting, high corrosion resistance in artificial saliva.

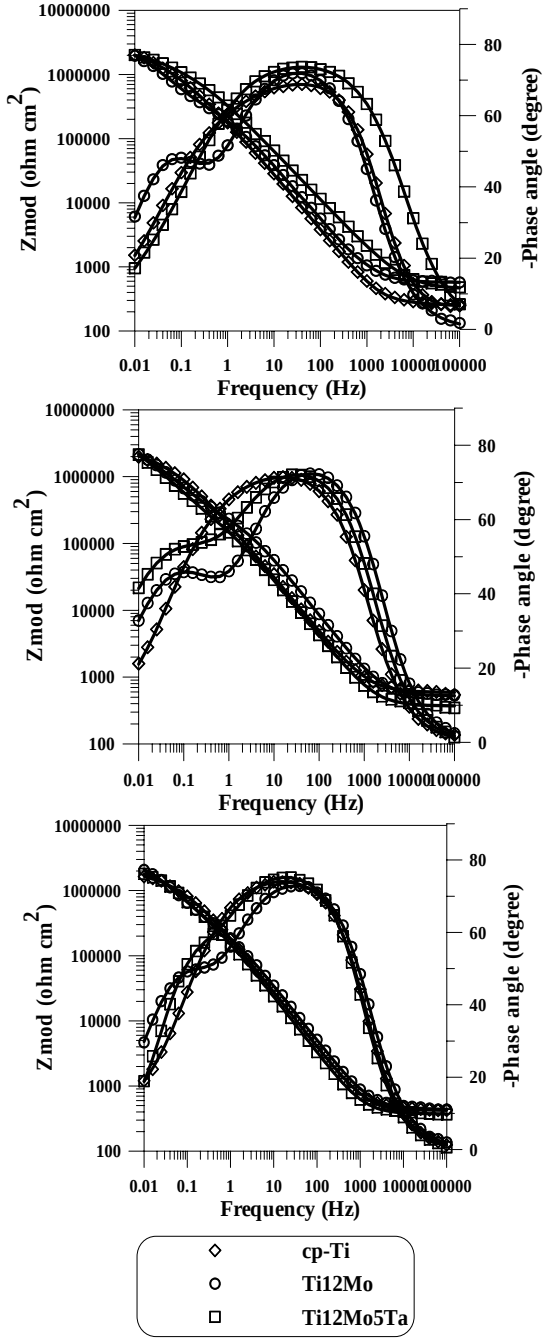

Fig. 4. Bode plots recorded for at selected potentials: (a) 0 V, (b) 0.5 V and (c) 1 V in artificial saliva, at 25 ^{o}C

For the interpretation of the electrochemical behaviour of a system from EIS spectra, an appropriate physical model of the processes occurring on the electrode (equivalent circuit) is necessary. Fitting of the impedance was done with an equivalent circuit (EC) using a series combination of the solution resistance, R_{sol} (about 100 Ω cm^2 for all cases), with two RQ elements in parallel: $R_{sol}(R_{oL}(Q_{oL}(R_{bL}Q_{bL})))$. Other combinations of resistance and capacitances were tried, in particular one RQ elements in parallel: $R_{sol}(R_{bL}Q_{bL})$ or two RQ parallel combinations: $R_{sol}(R_{oL}Q_{oL})(R_{bL}Q_{bL})$, to model the corrosion process of samples in artificial saliva, but none of these were found to give a satisfactory fit (values of chi-square (χ^2) test were about 10^{-2}).

The EC presented in Fig. 5 is based on a model used by *Pan et al.* [3] to simulated data in saline solution. These authors viewed the surface layer formed on titanium as a two-layer oxide, with an inner barrier layer and an outer porous layer. Studies performed on Ti-based alloys under physiological conditions showed that the EC proposed by *Pan et al*. [3] can be used successfully to describe the behaviour of these materials as well [4, 11, 45, 55-57]. The high-frequency parameters R_{oL} and Q_{oL} represent the properties of the reactions at the outer porous passive film/solution interface. The parameter R_{bL} coupled with Q_{bL} describes the processes at the inner barrier layer at the electrolyte/compact passive film interface. The values of fitted parameters of the EC are presented in Table 3.

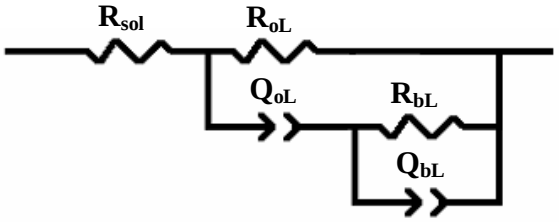

Fig. 5. Equivalent circuit (EC) used to fit the impedance data

Table 3. Values of fitted parameters of the equivalent circuits as function of applied potential Ti samples in artificial saliva.

Samples	E, V	10^6Q_{oL}, S cm^{-2} s^n	n_{oL}	$10^{-4}R_{oL}$, Ω cm^2	10^6C_{oL}, F cm^{-2}	10^6Q_{bL}, S cm^{-2} s^n	n_{bL}	$10^{-6}R_{bL}$, Ω cm^2	10^6C_{bL}, F cm^{-2}
cp-Ti	0	13	0.87	0.3	8.1	9.5	0.84	1.9	16.6
	0.5	9.4	0.87	2.5	7.6	8.9	0.84	2.0	15.5
	1	9.3	0.86	2.5	7.3	9.1	0.84	1.7	15.4
Ti12Mo	0	9.5	0.85	2.2	7.2	9.3	0.83	2.0	16.8
	0.5	9.1	0.85	2.1	6.8	8.7	0.83	2.1	15.7
	1	8.7	0.86	2.1	6.7	8.9	0.84	1.9	15.3
Ti12Mo5Ta	0	9.4	0.81	6.2	8.2	9.1	0.84	2.1	16.0
	0.5	9.5	0.85	2.6	7.5	8.6	0.84	2.3	15.1
	1	8.6	0.86	4.4	7.3	8.9	0.85	2.0	14.7

In the Fig. 4(a-c), the experimental data are shown as individual points, while the theoretical spectra resulted from the fits with a relevant EC model are shown as lines. In order to compare capacitance values for all the samples at different potentials, CPE for both layers, denoted as Q_{oL} and Q_{bL}, were recalculated, using equation [11, 58]:

$$C = \left(R^{1-n}Q\right)^{\frac{1}{n}} \tag{2}$$

High values of R_{bL} (order of 10^6 Ω cm^2) are observed at all potentials for all the samples, confirming the formation of a compact layer with high corrosion protection ability. R_{bL} was greater than R_{oL} by a factor of nearly 100 (Table 3) showing that the resistance of the oxide film on the all the sample and at all imposed potentials is due to this layer. R_{oL} remains relatively around 10^4 Ω cm^2, for all the samples, at all imposed potentials. Values of C_{oL} are smaller then those of C_{bL}, for all the samples, at all imposed potentials (Table 3). The slowly decrease in C_{oL} and C_{bL} starting from 0 V to 1 V, can be attributed to thickening of the oxide porous and oxide compact layers, because,

$$C = \frac{\varepsilon\varepsilon_o s}{l} \tag{3}$$

where *s* is the effective surface, ε is the dielectric constant for the passive film, ε_o the permissivity of free space, and *l* is the thickness. Another explanation might be that the effective surface, *s*, has increased.

According to the proposed model, the passive film consists of two layers, the inner barrier (compact) layer, R_{bL} and the outer porous layer, R_{oL}. The overall polarization resistance R_p is represented by the sum of partial resistance (R_{bL} + R_{oL}) [11]. R_p related to the rate of corrosion reaction(s) and is inversely proportional to the corrosion current; the Stern-Geary equation [59]:

$$i_{corr} = \frac{B}{R_p} \tag{4}$$

with B constant determined by Tafel slope tests.

As the potential changes from 0 V to 0.5 V, R_p increases and the C_{oL} and C_{bL} decrease. These results seem to correspond to a thickening of the titanium passive film. As the potential increases from 0.5 V to 1 V the R_p decreases slowly. The decrease in resistance indicates that the oxide layer may become more defective at large over potential [8, 56]. But, the R_p, of all the samples, in artificial saliva was large at 1 V (order of 10^6 Ω cm^2) as seen in Table 3. For highly corrosion resistance materials the R_p may even reach 10^6 Ω cm^2 [60]. This indicates that the samples are still highly resistant to corrosion even at large over potentials. The higher R_p of Ti12Mo alloy at all imposed potential indicates that this alloy possesses a superior corrosion resistance than cp-Ti in artificial saliva, and the addition of Ta for it improve this resistance.

In terms of EIS analysis, the corrosion resistance of titanium samples immersed in artificial saliva is improved with addition of Mo to cp-Ti. The addition of Ta for Ti12Mo alloy improves this resistance. Probable the decrease of α-phase proportion leads to improvement of corrosion behaviour of the Ti12Mo and Ti12Mo5Ta alloys. The addition of Ta probable stabilizes β-phases and this exhibits a nobler characteristic. The additions of the Mo and Ta have a positive contribution in the formation of the passive oxide film.

4. Conclusions

The electrochemical corrosion behaviour of Ti12Mo and Ti12Mo5Ta alloys in artificial saliva were investigated in this study. The following conclusions can be obtained.

(1) Open circuit potentials of the Ti12Mo and Ti12Mo5Ta alloys in artificial saliva are more electropositive than the cp-Ti due to beneficial effect of the alloying elements.

(2) Very low corrosion current densities were obtained indicating a high resistance for all the samples in artificial saliva.

(3) The EIS results of the samples in artificial saliva can be fitted using the model of $R_{sol}(R_{oL}(Q_{oL}(R_{bL}Q_{bL})))$. These results confirming the presence of a two layer film consisting of an inner barrier responsible for the corrosion protection, and an outer porous layer on the surface of the samples in artificial saliva.

(4) Values of polarization resistance indicate that the Mo used as alloying element improve the electrochemical corrosion behaviour of Ti12Mo alloys in artificial saliva, compared to the cp-Ti. The addition of Ta for Ti12Mo alloy improves this resistance.

References

[1] D. F. Williams, Biocompatibility of clinical implant materials. In: D.F. Williams, editor. Biocompatibility of clinical implant materials, vol.1, CRC Press, Boca Raton (1981).

[2] P. Kovacs, J.A. Davidson, Chemical and electrochemical aspects of the biocompatibility of titanium and its alloys. In: S.A. Brown, J.E. Lemons, editors. Medical applications of titanium and its alloys: the materials and biological issues. ASTM STP 1272. West Conshohocken: ASTM, (1996).

[3] J. Pan, D. Thierry, C. Leygraf, Electrochim. Acta **141**, 1143 (1996).

[4] J. E. G. Gonzalez, J. C. Mirza Rosca, J. Electroanal. Chem. **471**, 109 (1999).

[5] S. A. Shabalovskaya, G. C. Rondelli, A. L. Undisz, J. W. Anderegg, T. D. Burleigh, M. E. Rettenmayr, Biomaterials **30**, 3662 (2009).

[6] H.S. Kim, S. H. Lim, I. D. Yeo, W. Y. Kim, Mater. Sci. Eng. A **449–451**, 322 (2007).

[7] F. Contu, B. Elsener, H. Bohni, Corrosion Sci. **46**, 2241 (2004).

[8] S. L. Assis, S. Wolynec, I. Costa, Electrochim. Acta **51**, 1815 (2006).

[9] D. Mareci, R. Chelariu, D.M. Gordin, G. Ungureanu, Th. Gloriant, Acta Biomater. **5**, 3625 (2009).

[10] M. Metikos-Hukovic, A. Kwokal, J. Piljac, Biomaterials **24**, 3765 (2003).

[11] I. Milosev, T. Kosec, H.H. Strehblow, Electrochim. Acta **53**, 3547 (2008).

[12] C. N. Elias, Y. Oshida, J. H. Cavalcante Lima, C. A. Muller, J. Mech. Behav. Biomed. Mater. **1**, 234 (2008).

[13] R .A. Zavanelli, G. P. E. Herriques, I. Ferreira, M. D. A. Rollo, J. Prosthet. Dent. **84**, 274 (2000).

[14] C. Sitting, M. Textor, N. D. Spencer, M. Wieland, P. H. Vallotton, J. Mater. Sci. Mater. M. **10**, 35 (1999).

[15] W. F. Ho, W. K. Chen, S. C. Wu, H. C. Hsu, J. Mater. Sci. Mater. M. **19**, 3179 (2008).

[16] Y. Okazaki, E. Gotoh, Biomaterials **26**, 11 (2005).

[17] D. Kuroda, M. Niinomi, M. Morinaga, Y. Kato, T. Yashiro, Mater. Sci. Eng. A. **243**, 244 (1998).

[18] T. I. Kim, J. H. Han, I. S. Lee, K. H. Lee, M. C. Shin, B. B. Choi, Bio-Med. Mater. Eng. **7**, 253 (1997).

[19] Y. Okazaki, Y. Ito, K. Kyo, T. Tateishi, Mater. Sci. Eng. A. **213**, 138 (1996).

[20] S. Rao, Y. Okazaki, T. Tateishi, T. Ushida, Y. Ito, Mater. Sci. Eng. **C 4**, 311 (1997).

[21] G. He, J. Eckert, Q.L. Dai, M.L. Sui, W. Loser, M. Hagiwara, E. Ma, Biomaterials **24**, 5115 (2003).

[22] D. M. Gordin, E. Delvat, R. Chelariu, G. Ungureanu, M. Besse, D. Laillé, T. Gloriant, Adv. Eng. Mater. **10**, 714 (2008).

[23] M. Niinomi, Sci. Technol. Adv. Mater. **4**, 445 (2003).

[24] L. de Rosa, C.R. Tomachuk, J. Springer, D. B. Mitton, S. Saiello, F. Bellucci, Mater. Corros. **55**, 602 (2004).

[25] C. R. Tomachuk, L. de Rosa, J. Springer, D. B. Mitton, S. Saiello, F. Bellucci, Mater. Corros. **55**, 665 (2004).

[26] K. V. Rajagopalan, Annu. Rev. Nutr. **8**, 401 (1988).

[27] S. Kumar, T.S.N. Sankara Narayanan, J. Dent. **36**, 500 (2008).

[28] M. Niinomi, J. Mech. Behav. Biomed. Mater. **1**, 30 (2008).
[29] M. C. R. Alvez Rezende, A. P. Rosifini Alvez, E. N. Codaro, C.A. Matsumoto Dutra, , J. Mater. Sci. Mater. M. **18**, 149 (2007).
[30] N. T. C. Oliveira, A. C. Gustaldi, Corrosion Sci. **50**, 938 (2008).
[31] N. T. C. Oliveira, A. C. Gustaldi, Acta Biomater. **5**, 399 (2009).
[32] E. Eisenbarth, D. Velten, M. Muller, R. Thull, J. Breme, Biomaterials. **25**, 5705 (2004).
[33] Y. L. Zhou, M. Niinomi, T. Akahori, Mater. Sci. Eng. A. **371**, 283 (2004).
[34] Y. L. Zhou, M. Niinomi, T. Akahori, Mater. Sci. Eng. A. **384**, 92 (2004).
[35] Y. L. Zhou, M. Niinomi, T. Akahori, H. Fukui, H. Toda, Mater. Sci. Eng. A. **398**, 28 (2005).
[36] T. Zhou, M. Aindow, S. P. Alpay, M. J. Blackburn, M. H. Wu, Scr. Mater. **50**, 343 (2004).
[37] L. C. Zhang, T. Zhou, M. Aindow, S. P. Alpay, M. J. Blackburn, J. Mater. Sci. **40**, 2833 (2005).
[38] Y. Yang, W. Wang, F. Li, W.Li, Y. Zhang, Mater. Sci. Forum. **618-619**, 169 (2009).
[39] Gerd Liitjering, James C. Williams, Titanium, Springer-Verlag, Berlin Heidelberg (2003).
[40] P. Prioteasa, N. Ibris, T. Visan, J. Optoelectron. Adv. Mater. **9**, 3405 (2007).
[41] E. Gatin, C. Berlic, B. Iordache, P. Prioteasa, J. Optoelectron. Adv. Mater. **11**, 1870 (2009).
[42] D. M. Gordin, T. Gloriant, G. Texier, I. Thibon, D. Ansel, J.L. Duval, M.D. Nagel, J. Mater. Sci. Mater. M. **15,** 885 (2004).
[43] D. M. Gordin, T. Gloriant, Gh. Nemtoi, R. Chelariu, N. Aelenei, A. Guillou, D. Ansel, Mater. Lett. **59**, 2936 (2005).
[44] F. Cortial, Metall. Mater. Trans A. **25**, 241 (1994).
[45] D. Mareci, G. Ungureanu, D. Aelenei, J. C. Mirza Rosca, Mater. Corros. **11**, 848 (2007).
[46] J. F. McCabe, Applied dental materials, Blackwell Science Publication 7th edn., Oxford (1994).
[47] T. Fusayama, T. Katayori, S. Nomoto, J. Dent. Res. **42**, 1183 (1963).
[48] E. Vasilescu, P. Drob, D. Raducanu, I. Cinca, D. Mareci, J.M. Calderon Moreno, M. Popa, C. Vasilescu, J.C. Mirza Rosca, Corrosion Sci. **51**, 2885 (2009).
[49] I. D. Raistrick, J. R. MacDonald, D. R. Francschetti, Impedance Spectroscopy Emphasizing Solid Materials and Systems, John Wiley&Sons, New York (1987).
[50] G. Airoldi, G. Riva, M. Vanelli, V. Filippi, G. Garattini, Am. J. Orthod. Dentofac. Orthop. **112**, 58 (1997).
[51] E. Pelaez-Abellan, L. Rocha-Sousa, W. D. Muller, A. C. Guastaldi, Corrosion Sci. **49**, 1645 (2007).
[52] M. Pourbaix, Atlas of Electrochemical Equilibria in Aqueous Solutions, Pergamon Press, New York (1966).
[53] H. Schmidt, G. Stechemesser, J. Witte, M. Soltani-Farshi, Corrosion Sci. **40**, 1533 (1998).
[54] J. S. L. Leach, B.R. Pearson, Corrosion Sci. **28**, 43 (1988).
[55] A. Cremasco, W.R. Osorio, C.M.A. Freire, A. Garcia, R. Caram, Electrochim. Acta. **53**, 4867 (2008).
[56] I. C. Lavos-Valereto, S. Wolynec, I. Ramires, A. C. Guastaldi, I. Costa, J. Mater. Sci. Mater. M. **15**, 55 (2004).
[57] N. Ibris, J.C. Mirza Rosca, J. Electroanal. Chem. **526**, 53 (2002).
[58] D. Kek-Merl, L. Lappalainen, H.L. Tuller, J. Electrochem. Soc. **153**, J15 (2006).
[59] M. Stern, A. Geary, J. Electroch. Soc. **104**, 56 (1957).
[60] F. Mansfeld, J.Electrochem. Soc. **120**, 515 (1973).

*Corresponding author: sutiman@ch.tuiasi.ro